Energy Flow in an Atom Exchange Chemical Reaction in Solution

Ilan Benjamin, Bradley J. Gertner, Nina J. Tang, and Kent R. Wilson*

Contribution from the Department of Chemistry B-039, University of California, San Diego, La Jolla, California 92093-0339. *Received May 1, 1989*

Abstract: The object of this paper is to help understand the role of energy fluctuation and transfer in thermally activated chemical reactions in solution. We examine the path of energy flow through the different modes of the solvent and the reagents via molecular dynamics simulation of a model atom exchange reaction in rare gas solution. We follow the energy ultimately needed to surmount the activation barrier from its origin in the heat bath of the solvent through the sequence of (i) an initial fluctuation involving the high translational excitation of a few solvent atoms adjacent to the reactants, (ii) hard solvent–reactant collisions producing potential energy spikes, (iii) the appearance of kinetic (translational and some rotational) energy in the reactants, and finally (iv) an "internal collision" between the reactants converting their excess kinetic energy into potential energy as the barrier is surmounted. The time scale of the entire energy flow process is ~250 fs. The role of momentum and kinetic energy is seen to be fundamental in understanding the molecular dynamic mechanism of this solution reaction, in contrast to the usual view of reaction mechanism which concentrates on potential energy and atomic positions.

I. Introduction

In recent years our understanding of the microscopic, molecular dynamic aspect of the *rates* of chemical reactions in solution has considerably improved.[1-11] The rate, however, is only one aspect of a chemical reaction. The general picture, the detailed molecular dynamic mechanism of how chemical reactions take place in solution, still remains to be fully explained. We do not yet understand, for example, the subject we consider in this article, the multimolecular processes in thermally activated solution reactions whereby energy flows from the solvent, through intermediate forms, into the reactants, ultimately appearing as potential energy at the barrier top.

We can view the mechanism of climbing the barrier in an activated chemical reaction in solution as a fluctuation in an equilibrium ensemble.[9,10,12,13] But while the thermodynamic theory of fluctuations is well developed, little is known about the dynamical nature of the actual fluctuations which are important for climbing the barrier in activated chemical reactions in a liquid. The actual fluctuations, as viewed in phase space, can involve momenta (i.e., kinetic energy fluctuations) as well as coordinates (i.e., potential energy fluctuations). For these fluctuations to be effective they must meet criteria defined both thermodynamically (the rareness of the fluctuation must match the amount of free energy needed to climb the free energy barrier), and dynamically (the fluctuation must mechanically arise from the particular Hamiltonian of the reacting system and must couple to the reaction coordinate to drive the reaction process[13]). In this paper we focus on the mechanical, dynamical aspects of the fluctuation, specifically how the energy necessary to climb the reaction barrier is transferred and transformed. To investigate this, we choose the $Cl + Cl_2 \rightarrow Cl_2 + Cl$ reaction in argon-like solvent at room temperature, which has been used previously[1,14] in studies of solution–reaction dynamic effects on rates and energy flow within and into the solute.

Clearly, the energy must initially come from the heat bath of the solvent, and must be great enough to surmount the energy barrier. The scale of the energy flow fluctuation can be indicated by an analogy. If one imagines a fictitious process in which a mole of reactants synchronously passes over the 84-kJ/mol (20-kcal/mol) energy barrier illustrated here during the ~250 fs we observe, the power required to flow from the solvent to the reactants would be $\sim 10^5$ times all the electric power generated on earth.[15] A question which is both interesting and answerable in terms of computer simulation is, "What is the specific energy transfer mechanism and series of modes through which the energy is passed from the solvent to the reaction system at the barrier to?" Is it mainly through transfer of kinetic energy or mainly through potential energy? Is the energy flow through single hard sphere collisions with a few solvent atoms or does it require the cooperation of many such atoms positioned in a particular way? The answers to such questions can be expected to depend upon the specific nature of the reactants and the solvent. For example, in charge-transfer reactions in polar solvents, where long-range forces are involved, the energy flow mechanism may be quite different from that in a reaction between neutral species in a rare gas solvent, as illustrated here. In what follows it will often be useful, particularly since this is a symmetrical reaction in which the reactants are the same as the products, to keep in mind that the arising of the fluctuation by which the barrier is climbed by the reactants is just the time reversal of the fluctuation decay process[16] by which the products dissipate their "specialness".

The barrier climbing process exhibits a simple yet revealing picture of the exchange of energy from the solvent, through a series of different modes, to the reactants, ending up as reagent potential energy at the top of the barrier. The transition from a pseudo-equilibrium at −500 fs to pseudo-equilibrium at +500 fs starts with a "heat wave" of excess thermal energy flowing from the surroundings into a "hot spot" region of solvent near the reactants and then into a few solvent atoms adjacent to the reactants and is transformed within ~250 fs through a few hard solvent–reactant collisions, largely into translational and some rotational energy in the reactants. Then the kinetically excited reactants collide with one another and convert their excess thermal energy into

* Author to whom inquiries about the paper should be addressed.

(1) Paper I: Bergsma, J. P.; Reimers, J. R.; Wilson, K. R.; Hynes, J. T. *J. Chem. Phys.* **1986**, *85*, 5625 (BRWH).
(2) Bergsma, J. P.; Gertner, B. J.; Wilson, K. R.; Hynes, J. T. *J. Chem. Phys.* **1987**, *86*, 1356.
(3) Hynes, J. T. In *Theory of Chemical Reaction Dynamics*; Baer, M., Ed.; CRC Press: Boca Raton, FL, 1985; Vol. IV, and references therein.
(4) Chandler, D. *J. Chem. Phys.* **1978**, *68*, 2959.
(5) Montgomery, J. S., Jr.; Chandler, D.; Berne, B. J. *J. Chem. Phys.* **1979**, *70*, 4056.
(6) Rosenberg, R. O.; Berne, B. J.; Chandler, D. *Chem. Phys. Lett.* **1980**, *75*, 162.
(7) Allen, M. P.; Schofield, P. *Mol. Phys.* **1980**, *39*, 207.
(8) Adelman, S. A. *Adv. Chem. Phys.* **1983**, *53*, 61.
(9) Warshel, A. *J. Phys. Chem.* **1982**, *86*, 2218.
(10) Warshel, A.; Hwang, J.-K. *J. Chem. Phys.* **1986**, *84*, 4938.
(11) Gertner, B. J.; Wilson, K. R.; Hynes, J. T. *J. Chem. Phys.* **1989**, *90*, 3537, and references therein.
(12) Hwang, J.-K.; King, G.; Creighton, S.; Warshel, A. *J. Am. Chem. Soc.* **1988**, *110*, 5297.
(13) Wilson, K. R.; Levine, R. D. *Chem. Phys. Lett.* **1988**, *152*, 435.
(14) Bergsma, J. P.; Edelsten, P. M.; Gertner, B. J.; Huber, K. R.; Reimers, J. R.; Wilson, K. R. Wu, S. M.; Hynes, J. T. *Chem. Phys. Lett.* **1986**, *123*, 394.
(15) Of course, the actual climbing is done at random and only ~ $\exp(-E_a/kT)$ of the reagents will, at any given moment, be near the barrier top.
(16) Ohmine, I. *J. Chem. Phys.* **1986**, *85*, 3342.

0002-7863/90/1512-524$02.50/0

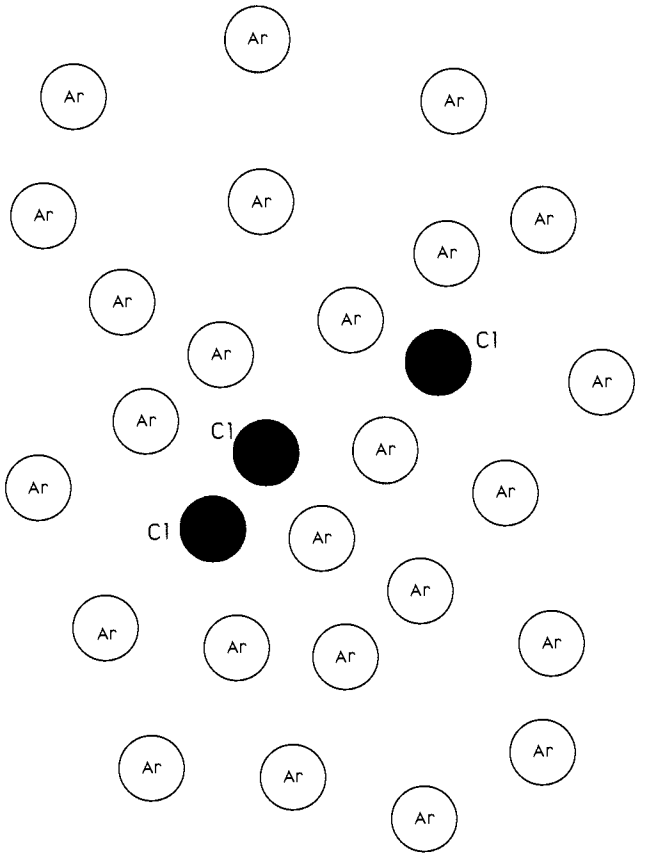

Figure 1. the Cl + Cl_2 → Cl_2 + Cl reaction model in fluid argon solvent. One hundred Ar atoms are used in the actual simulations.

reagent potential energy as the system reaches the top of the barrier. As has been described elsewhere,[1] in this reaction system (i) there are almost no barrier recrossing and thus transition-state theory gives the correct reaction rate, and (ii) the flow of energy from the solvent into reactant vibrational excitation (which is also used to help climb the energy barrier) occurs on a much longer time scale than that of our simulations.

In order to investigate the energy flow process, we use molecular dynamics simulation. To facilitate the simulation, we apply the usual method of initiating trajectories at the barrier top. The general validity of this method has been demonstrated using detailed-balance arguments,[17,18] in particular for the purpose of calculating rate constants. Thus, we simulate the fluctuation process of climbing the reaction barrier by looking at the reverse, energy dissipation, process. In earlier articles[1,14] the energy flow within the reagents themselves is illustrated. In the present article we extend our investigation to consider the origin and evolution of the reaction energy in the solvent and the means by which it is transferred from the solvent to the reactants. While the results presented here are specific to this system, we believe that the insights gained are useful in understanding energy flow in other reactions.

The paper is organized as follows. In section II we describe the system used in the molecular dynamics simulation and the method used to collect and analyze the data. In section III we present and discuss the results, and we conclude in section IV with general remarks.

II. Methodology and the Hamiltonian

A. System Potentials. Because the details of the reaction system have been presented in another article by Bergsma, Reimers, Wilson, and Hynes,[1] which we will call BRWH, we only summarize them briefly here. Our trajectories are modeled after a simple A + BC → AB + C atom-transfer reaction in solution, with the triatomic solute represented by chlorine-like atoms of mass 35, and the solvent by 100 argon-like atoms at a density[19] of 1.4 g cm^{-3} (see Figure 1).

The potential energy for the system is given by a sum of solvent, solute, and solvent–solute terms. The solvent potential energy is assumed to be a sum of pair interactions between solvent atoms. Each pair interaction between solvent atoms i and j is taken to be a Lennard-Jones 6–12 potential

$$\Phi_{\text{solvent}} = \sum_{i<j} \Phi^{\text{LJ}}(r_{ij}) \qquad \text{(II.1)}$$

$$\Phi^{\text{LJ}}(r_{ij}) = 4\epsilon_{ij}\left[\left(\frac{\sigma_{ij}}{r_{ij}}\right)^{12} - \left(\frac{\sigma_{ij}}{r_{ij}}\right)^{6}\right]$$

where r_{ij} is the distance between the two atoms, ϵ_{ij} is the depth of the minimum in the potential, and σ_{ij} determines the finite intermolecular distance at which $\Phi^{\text{LJ}}(r_{ij}) = 0$. The values of ϵ_{ij} and σ_{ij} are given in BRWH. The ABC solute–solute reagent potential energy is represented by a three-body London–Eyring–Polyani–Sato (LEPS)[20] surface, Φ^{LEPS}, which is described in detail in BRWH. The reagent potential energy asymptotically reduces to a diatomic bound Morse potential[21] when one chlorine atom separates from the other two. The parameters chosen for this potential define a sharp barrier with a height of 84 kJ/mol (20 kcal/mol). Finally, the solvent–solute potential energy term is represented by a sum of pair interactions between solvent atom i and solute atom ν, each taken to be a Lennard-Jones 6–12 potential

$$\Phi_{\text{solvent-solute}} = \sum_{i,\nu} \Phi^{\text{LJ}}(r_{i\nu}) \qquad \text{(II.2)}$$

with constants $\epsilon_{i\nu}$ and $\sigma_{i\nu}$ as given in BRWH.

B. Molecular Dynamics. The periodic boundary conditions of our system are defined by a truncated octahedron[22] (bcc unit cell with lattice constant $a/2$ = 10.67 Å), so as to approximate an infinite fluid argon solvent. To determine the molecular dynamics of the 103 solute and solvent atoms involved, we use Hamilton's equations of motion for particles in a conservative force field

$$\dot{\mathbf{r}}^N = \frac{\partial H}{\partial \mathbf{p}^N}, \quad \dot{\mathbf{p}}^N = -\frac{\partial H}{\partial \mathbf{r}^N} \qquad \text{(II.3)}$$

where $\mathbf{p}^N$ and $\mathbf{r}^N$ are the conjugate momentum and position coordinates for a system of N particles, and H is the Hamiltonian of the system, given by

$$H = K_{\text{solute}} + K_{\text{solvent}} + \Phi^{\text{LEPS}} + \Phi_{\text{solvent}} + \Phi_{\text{solvent-solute}} \qquad \text{(II.4)}$$

where the K's are the kinetic energies, and the potential energies are as defined above. A maximum range of 8 Å is used for the potentials, and force discontinuities are avoided by feathering the potentials smoothly to zero.[2,23,24] We numerically integrate these classical equations of motion using a modified Verlet algorithm[23,25–27] with a time step of 1.0 fs.

C. Initial Conditions and Trajectories. Our trajectories are initiated from the top of the barrier, i.e., at the transition state, then run forward and backward in time. This technique, developed by Keck,[28] Anderson,[17,18] and Bennett,[29,30] is more practical than beginning trajectories far from the transition state because it alleviates the problem of infrequent successful reactions caused by high energy of activation, and thus maximizes the efficiency of the simulations.

We begin by preparing 10 independently chosen initial seed configu-

(17) Anderson, J. B. *J. Chem. Phys.* **1973**, *58*, 4684.
(18) Anderson, J. B. *J. Chem. Phys.* **1975**, *62*, 2446.

(19) This corresponds to a liquid density at lower temperature. We study the system at 298 K, above the critical point for Ar.
(20) Kuntz, P. J. In *Dynamics of Molecular Collisions, Part B*; Miller, W. H., Ed.; Plenum: New York, 1976, p 53.
(21) Huber, K. P.; Herzberg, G. *Constants of Diatomic Molecules*; Van Nostrand Reinhold: New York, 1979.
(22) Adams, D. J. In *The Problem of Long-Range Forces in the Computer Simulation of Condensed Media*; Ceperly, D., Ed.; National Resource for Computation in Chemistry: Berkeley, 1980; p 13.
(23) Swope, W. C.; Andersen, H. C.; Berens, P. H.; Wilson, K. R. *J. Chem. Phys.* **1982**, *76*, 637.
(24) Andrea, T. A.; Swope, W. C.; Andersen, H. C. *J. Chem. Phys.* **1983**, *79*, 4576.
(25) Allen, M. P.; Tildesley, D. J. *Computer Simulation of Liquids*; Clarendon Press: Oxford, 1987.
(26) Beeman, D. *J. Comput. Phys.* **1976**, *20*, 130.
(27) Hockney, R. W.; Eastwood, J. W. *Computer Simulation Using Particles*; Mc-Graw-Hill: New York, 1981.
(28) Keck, J. C. *Discuss. Faraday Soc.* **1962**, *33*, 173.
(29) Bennett, C. H. In *Diffusion in Solids*; Burton, J. J., Ed.; Academic: New York, 1975; p 73.
(30) Bennett, C. H. In *Algorithms for Chemical Computations*; Christofferson, R. E., Ed.; ACS Symposium Series 46; American Chemical Society: Washington, DC, 1977; p 63.

rations of the solvent and solute atoms by selecting their positions at random, checking that no atoms are too close to one another. Each one of these "seeds" is energy minimized subject to the constraint that the triatomic (ABC) solute is at the transition state, defined such that the ABC asymmetric stretch is zero; i.e., the AB distance equals the BC distance. From each of the 10 seeds, 10 different initial conditions are prepared by equilibrating the system at a temperature of 298 K, while the solute is at the transition state, free to move in its symmetric stretch and bend coordinates, as well as to rotate and translate as a whole. Thus, the 100 initial condition files are selected from a canonical ensemble of systems at the transition state.

Each initial condition file is used to initiate a trajectory from the top of the barrier at time $t = 0$ by removing the constraint that the asymmetric stretch of ABC is set to zero and by selecting all velocities from a Maxwell–Boltzmann distribution at 298 K. Trajectories are propagated using a constant energy algorithm for a half-picosecond in both the positive and negative time directions. As the reaction progresses, the resulting positions, momenta, kinetic and potential energies, and cumulative work done by the solvent atoms on the reactants are collected at 10-fs intervals. For any given solvent atom j, a solvent–solute potential energy is calculated as a function of time as the sum of its potential relative to each of the three solute atoms, $\Phi_j = \sum_\nu \Phi^{LJ}(r_{j\nu})$. The work ΔW done by each solvent atom j is defined, for our purposes, by looking at the trajectory starting at $\tau = -500$ fs, and integrating,

$$\Delta W_j(t) = \int_\tau^t \sum_\nu \mathbf{f}_{\nu j}(t') \cdot \dot{\mathbf{r}}_\nu(t')\, \mathrm{d}(t') \qquad \text{(II.5)}$$

where t is a time during the reaction, $\mathbf{f}_{\nu j}$ is the force exerted on chlorine solute atom ν by solvent atom j, and $\dot{\mathbf{r}}_\nu$ is the velocity of the chlorine atom involved. The sum of all the $\Delta W_j(t)$ over the solvent atoms j is the total work done by the solvent on the reagents, and it must equal the change in the energy of the reagents[31]

$$\sum_j \Delta W_j(t) = E_{\text{solute}}(t) - E_{\text{solute}}(\tau) \qquad \text{(II.6)}$$

which is on the average approximately[32] the gas-phase barrier height as $\tau \to -\infty$ and with $t = 0$. We also record the position of each solvent atom in terms of its distance relative to the reagents and, in particular, whether the solvent atom under consideration is nearer the Cl atom or the Cl_2 molecule.

We collect these data for 100 trajectories to achieve reasonable statistics. Because we consider them both as averages over the entire ensemble of trajectories and on an individual basis, we are able to directly observe in the simulation the nature of those energy fluctuations which result in successful reactions.

III. Results

At the origin of each of our 100 trajectories (which represent a sample of reactive trajectories) where time $\tau = -500$ fs, we begin with essentially all the energy thermally distributed in the kinetic and potential energy of the solvent. As we near the middle of the trajectory, i.e., approaching $t = 0$, the solute potential energy rises as the barrier is surmounted. Our interest is in what transpires between these two points in time, resulting in the conversion of solvent thermal energy to potential energy of the reagents at the top of the barrier.[33] By separately observing the evolution in time of the modes of solvent kinetic and potential energies, solvent–reagent potential energy, work done by the solvent on the reagents, reagent translational and rotational energy, and reagent potential energy, we are able to observe the sequential flow of energy among these modes. We observe this energy flow both for individual trajectories and for an average over an ensemble of 100 trajectories.

A. Kinetic and Potential Energies of the Solvent "Hot Spot". Considering the ensemble of only those trajectories which will ultimately react, we observe that at a time sufficiently long before reaching the barrier top the energy is distributed in an approximately equilibrium fashion, mainly in the potential and kinetic energies of the solvent. Because of the finite number of solvent atoms and our microcanonical trajectories, the "temperature" at this point in our simulation is actually about 25 K higher than our temperature at 298 K at the barrier top. In experimental reality, a "heat wave" will flow in from the surrounding solution, and shortly before barrier climbing there will be a "hot spot" of excess thermal energy in the solvent in the vicinity of the reagents. This excess thermal energy will then flow from the solvent into the reagents. (Even with an infinite heat bath of solvent, an initial "hot spot" of solvent in the region of the nascent reaction, carried in by a "heat wave" from the surroundings, is expected, as this makes the reactive event more probable. This can be more clearly understood by considering the time-reversed process of dissipation of energy in falling off of the barrier.)

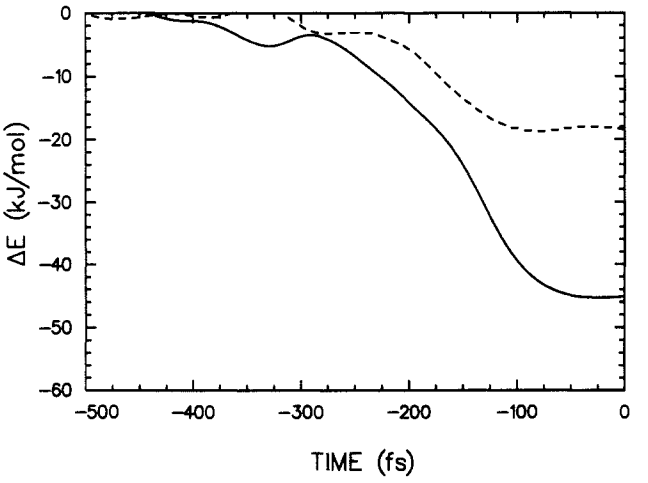

Figure 2. Change in the total kinetic (solid line) and potential (dashed line) energies of the solvent in the process of climbing the barrier, averaged over 100 trajectories. The zero of time is at the barrier top, and the zero of energy is set to the energy at −500 fs.

We first consider the change in the total solvent kinetic and potential energies from $\tau = -500$ fs to $t = 0$ fs at the barrier top. Figure 2 shows that most of the energy necessary for climbing the barrier results from excess kinetic energy of the solvent, with much less coming from the solvent–solvent potential energy. This can be understood in an approximate equilibrium context if we think about the contributions of kinetic and potential energies to the specific heat of a rare gas solvent. For a solvent with N particles, in a microcanonical ensemble, the constant volume heat capacity C_V is related to the fluctuations in the kinetic energy via[25,34]

$$\langle(\Delta K)^2\rangle_{NEV} = \tfrac{3}{2}Nk_B{}^2T^2(1 - 3Nk_B/2C_V) \qquad \text{(III.7)}$$

in which ΔK is the deviation of the kinetic energy from its average value, NEV indicates that the ensemble average is for constant particle number N, total energy E, and volume V, and k_B is Boltzmann's constant. The relation $K = 3Nk_BT/2$ can be used to rewrite this equation as

$$C_V = \tfrac{3}{2}Nk_B/(1 - 3N\langle(\Delta T)^2\rangle/2T^2) \qquad \text{(III.8)}$$

If we think about our reagents as an energy sink cooling the solvent, with $C_V \approx \Delta E/\Delta T$, then for a barrier of ΔE the change in the kinetic energy of the solvent will be

$$\Delta K = \tfrac{3}{2}Nk_B\Delta T = (1 - 3N\langle(\Delta T)^2\rangle/2T^2)\Delta E \qquad \text{(III.9)}$$

Using $\Delta E = \Delta K + \Delta\Phi$, where $\Delta\Phi$ is the deviation from the average of solvent potential energy, we have

$$\frac{\Delta K}{\Delta\Phi} = \frac{2T^2}{3N\langle(\Delta T)^2\rangle} - 1 \qquad \text{(III.10)}$$

The right-hand side can be calculated from an equilibrium microcanonical run of our system away from the barrier top. The result is $\Delta K/\Delta\Phi = 2.3 \pm 0.2$, which agrees with the ratio of energy

(31) Goldstein, H. *Classical Mechanics*, 2nd ed.; Addison-Wesley: Reading, MA., 1980.

(32) This is exact for a reaction system where the reaction coordinate is totally separable from other solute and solvent coordinates.

(33) In a reaction system with stronger coupling to the solvent, the energy change associated with climbing the barrier may also include a significant contribution from the change in reagent-solvent interaction along the reaction coordinate.

(34) Lebowitz, J. L.; Percus, J. K.; Verlet, L. *Phys. Rev.* **1967**, *153*, 250.

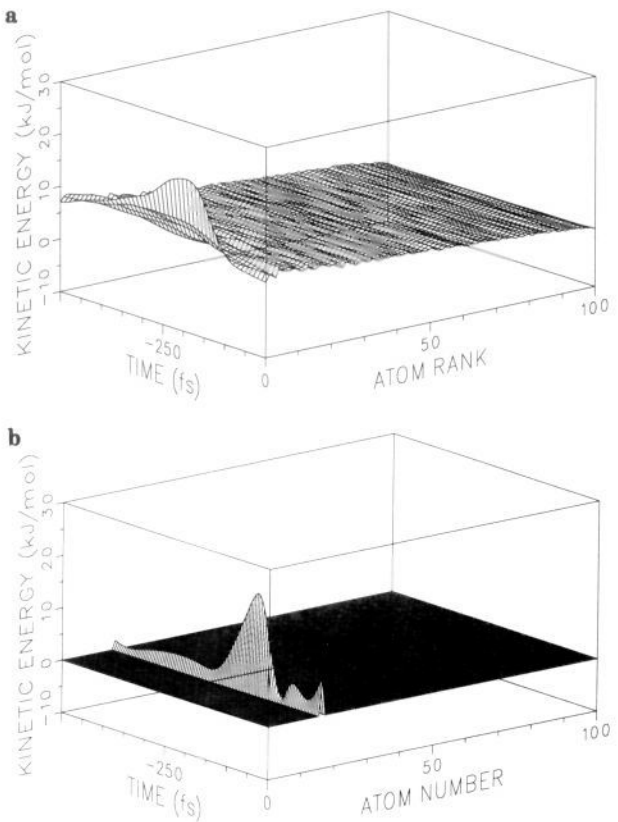

Figure 3. (a) Solvent kinetic energy as a function of time and atom rank, averaged over 100 trajectories. Atoms are ranked according to their maximum kinetic energy, as discussed in the text. (b) Time-dependent kinetic energy of the argon solvent atom having the greatest kinetic energy peak, shown for an individual trajectory. This atom is also the one with the highest maximum of solvent–solute potential energy and of work done on the reactants. Kinetic energies of the other solvent atoms are not shown.

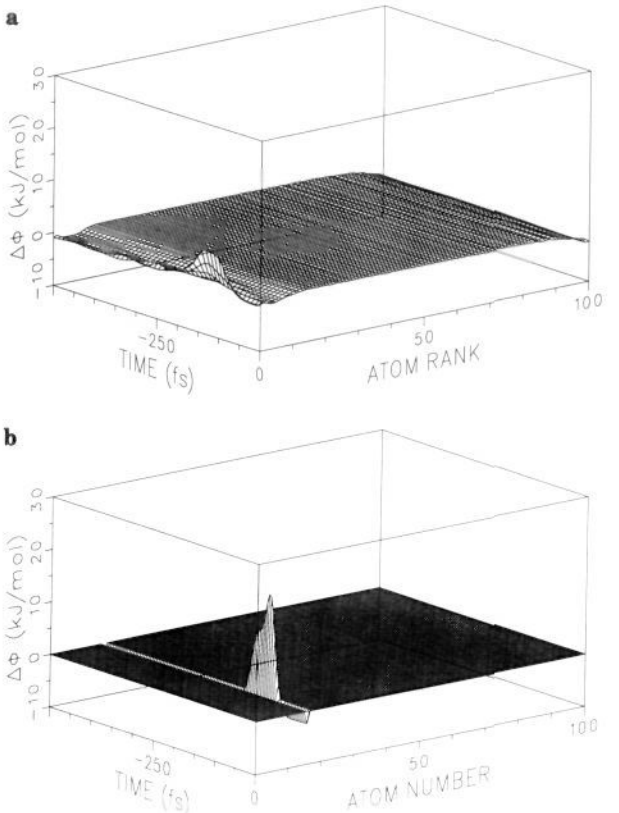

Figure 4. (a) Change in solvent–solute potential energy Φ as a function of time and atom rank, averaged over 100 trajectories. Atoms are ranked according to their maximum solvent–solute potential energy, as discussed in the text. (b) Time-dependent change in solvent–solute potential energy of the argon solvent atom having the greatest potential energy peak, shown for an individual trajectory. Potential energies of the other solvent atoms are now shown.

flow from solvent kinetic versus potential energy shown in Figure 2.

B. High Kinetic Energy in a Few Solvent Atoms. Next we look at the distribution of the solvent kinetic energy among the solvent atoms. For each trajectory we rank the solvent atoms according to the magnitude of the kinetic energy peak (atom 0 has the highest kinetic energy peak, atom 1 the second highest, which may occur at a different time, and so on). In Figure 3a we show the average over 100 trajectories of the kinetic energy of the solvent atoms ranked as explained above. A kinetic energy peak, involving only a few solvent atoms, occurs at approximately −200 fs, reaching a maximum of about 19 kJ/mol. Such a low value would seem to make it impossible for our 84-kJ/mol barrier to be crossed using this source of energy. However, by looking at randomly chosen individual trajectories we see that this deceptively low value is a result of averaging over our ensemble. For example, in Figure 3b we show, for one trajectory, the kinetic energy of the solvent atom having the largest peak in kinetic energy. Individual graphs show energy peaks of over 30 kJ/mol, which are shorter in time and reach higher values. Thus, individual solvent atoms in each trajectory (and in different trajectories) reach peaks at different times, and the peak of the average is not the average of the heights of individual solvent atom peaks taken irrespective of time of peaking. To summarize, although averaging broadens the distribution, starting at $t \approx -250$ fs, a few solvent atoms gain excess kinetic energy from the other solvent atoms.

C. Solvent–Solute Hard Collisions and Potential Energy Spikes. The peak in kinetic energy of a single solvent atom is promptly followed by a rapid decay of its kinetic energy, coinciding with a steep rise in solvent–solute potential energy for that solvent atom as it strikes either the reactant atom or diatomic. Many correlations may be noted between the kinetic and potential energy graphs. As seen in Figure 4a, the ensemble average potential energy increases to a peak of approximately 6 kJ/mol near −125 fs, and then dissipates rapidly within the next 100 fs, much as the kinetic energy did. Furthermore, like the kinetic energy graphs, the maximum value of potential energy attained by a solvent atom is lowered by our averaging over the ensemble, but may be revealed via graphs of individual trajectories. From Figure 4b, we see that maximum potential energy peaks are closer to the order of 18 kJ/mol than 6 kJ/mol of energy. We also note, in comparing Figure 3b and 4b for the individual trajectory that the solvent atom number with the greatest potential energy in Figure 4b is the same as that atom which attains maximum kinetic energy in Figure 3b. Clearly, crossing the barrier top is dependent upon the energy concentrated in a few specific solvent atoms, while the remaining atoms contribute much less to the energy required for the reaction. By −100 fs from the transition-state barrier, the few positive solvent–solute potential energy peaks have already diminished to negative values. Additional insight can be gained from calculating the work done by the solvent (viewed as an external force) upon the reagents.

D. Work Done by Solvent on Reagents. While the solvent kinetic and potential energy spikes are indicative of energy transfer in the solvent, they are not direct measures of the energy-transfer process behind successful barrier crossing. One direct measure is the work done on the reactants by the solvent. As the solvent–solute potential energy rises and decays, the solvent does work on the solute atoms both by accelerating them to high velocities and by pushing them up the reagent potential energy barrier. Hence, we see that the decline of the solvent–solute potential energy peak is accompanied by a rapid rise in the amount of work done on the reactants by the solvent (Figure 5a,b). Solvent atoms begin to do work on the reagents approximately 200 fs before the

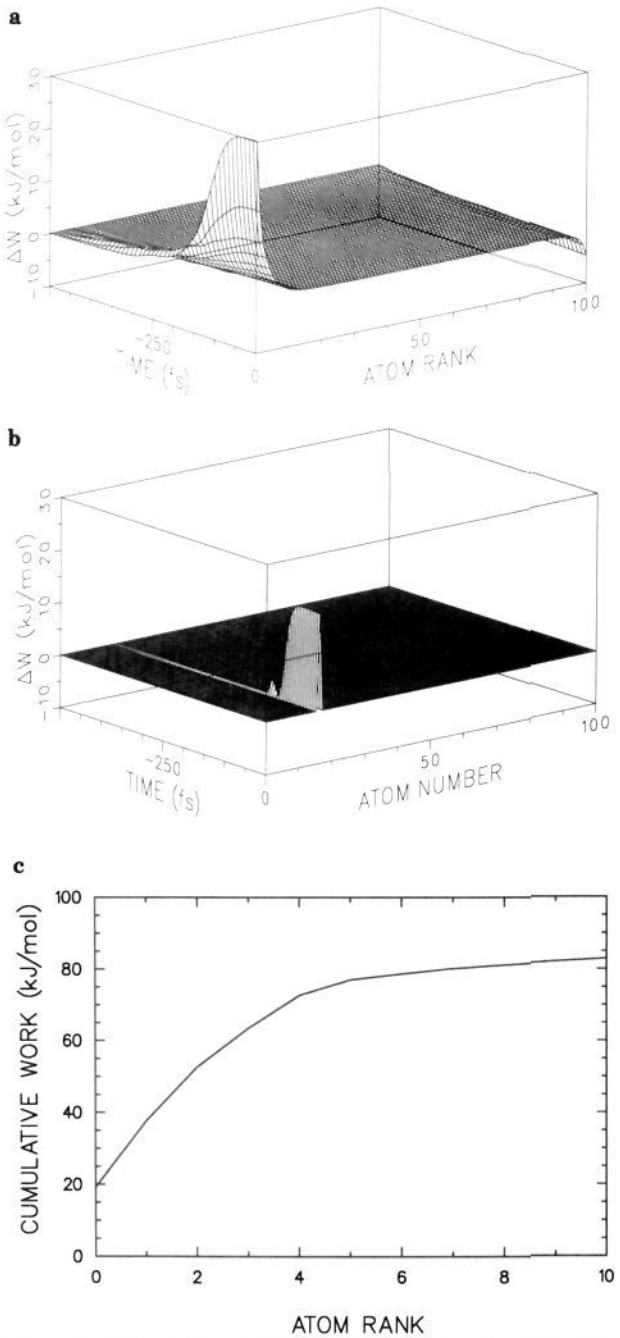

Figure 5. (a) Ranked work W done by the solvent on the solute, integrated from time $\tau = -500$ fs to the point where the barrier is crossed, and averaged over 100 trajectories. Atoms are ranked according to their maximum value of work done, as discussed in the text. Work is defined as being zero at −500 fs, far before the barrier is crossed, then integrated from that point on to time $t = 0$ at the barrier top. (b) Work done by the solvent atom having the maximum kinetic and solvent–solute potential energy as seen in Figure 3b and 4b. Of all the solvent atoms, this atom also does the greatest amount of work in driving the reaction over the barrier; the quanity of work done by other atoms is much less by comparison. Work done by other solvent atoms is not shown. (c) Cumulative work done by the solvent atoms on the reactants as a function of atom rank, averaged over 100 trajectories, illustrating that a few solvent atoms contribute almost all the work.

barrier and very rapidly reach a maximum of over 30 kJ/mol total work done by a single solvent atom. In Figure 5a we plot the work ΔW, defined in eq II.6, as a function of time and atom rank (atom 0 did the maximum work, etc). This work is averaged over 100 trajectories. In Figure 5b we show for a randomly chosen trajectory the work done as a function of time by the solvent atom

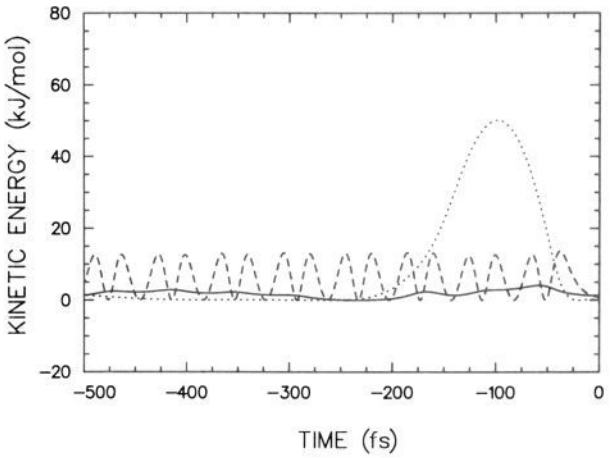

Figure 6. Translational, vibrational and rotational kinetic energies of the three Cl atoms as a function of time, shown for an example trajectory. The dotted line is Cl–Cl_2 relative translational energy, the dashed line is Cl_2 vibrational kinetic energy, and the solid line is Cl_2 rotational energy.

having the maximum kinetic and solvent–solute potential energies. From these two plots we see that work is done by a few solvent atoms, and is highly correlated with their kinetic and solvent–solute potential energies. By looking at the cumulative work done by the solvent atoms as a function of the atom rank (Figure 5c), we see that five liquid atoms contribute more than 90% of the work necessary to climb the 84-kJ/mol barrier.

We also examine the work done by each solvent atom in terms of its position in angle and distance relative to the reagents. By differentiating between those solvent atoms which interact with the diatomic Cl reactant and those which interact with the remaining atomic Cl, we may determine the distribution of the work done by the solvent in terms of their positions and how they affect the chlorine atoms such that the barrier is successfully crossed. (This is accomplished in part by viewing the 3D computer animated trajectories.) We find that, over the 100 trajectory ensemble, 75% of the five highest kinetic energy solvent atoms are closer to the Cl atom reactant than to the Cl_2 molecule. This can be understood as a mass effect since it is more efficient[31] for the argon atoms to transfer the necessary kinetic energy to the single atom of nearly equal mass than to a diatomic of almost twice the mass. Furthermore, the second- or third-highest kinetic energy solvent atoms tend to interact with either atom B or C of the diatomic such that the kinetic energy is transferred to both the translational and rotational energies of the diatomic which, as it swings into proper orientation, is then converted to reagent potential energy of barrier climbing. Thus, the fluctuation mechanism behind an acceptable reaction is such that (i) the kinetic energy transfer is sufficiently large and (ii) the excess momentum in the reactants is directed in such a way as to push the A and BC toward each other so as to end up in an approximately linear configuration. Since we are considering only the ensemble of accepted fluctuations, any deviation from equilibrium behavior results from the special mechanical constraints on the fluctuation necessary for climbing the barrier.

E. Reagent Translational, Rotational, and Vibrational Kinetic Energy. The picture of energy flow into and within the solute is already outlined in BRWH.[1] Here we briefly discuss it and draw the connection with the energy flow in the solvent. Approximately 100 fs before reaching the barrier top, the reagent atoms gain translational and rotational energy due to a few hard collisions with nearby solvent atoms. In Figure 6 we show, from an example trajectory, the time evolution of the total kinetic energy of the three solute atoms as partitioned into the relative translational energy of the atom relative to the diatomic, the rotation of the diatomic, and the vibrational energy of the diatomic. (The center of mass translation of the whole Cl_3 system is not shown.) The ensemble average rotational and translational energies start from near their equilibrium values at −500 fs, whereas the vibration

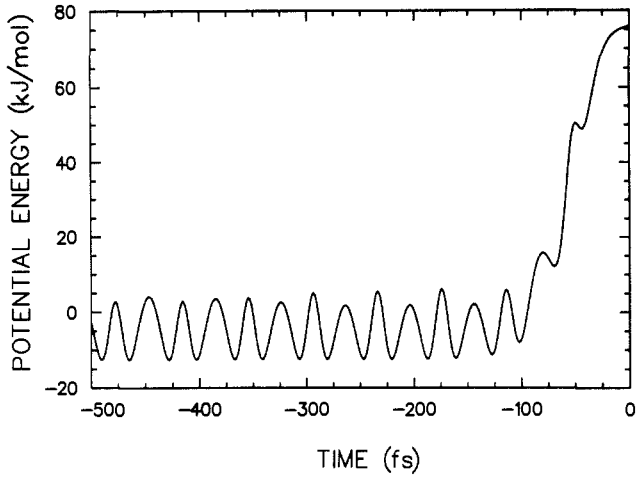

Figure 7. Internal potential energy of the three Cl atoms as a function of time, shown for the same trajectory as in Figure 6. The zero of potential energy is set at the −500 fs value.

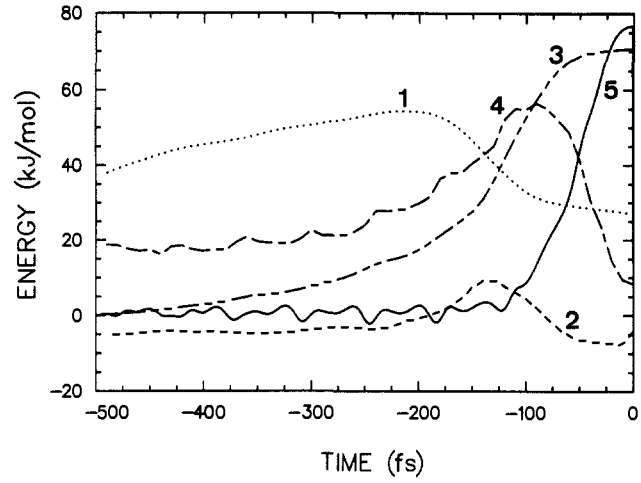

Figure 8. Energy flow showing the different energy modes and their time evolution (averaged over 100 trajectories). The different energies shown are (1) the sum of the kinetic energies of the five atoms which did the most work (dotted line), (2) the change in potential energy of these solvent atoms with respect to the reagent atoms (dashed), (3) the total accumulated work done by these solvent atoms on the reagents (double-short single-long-dashed), (4) the total internal kinetic energy of the Cl_3 system (double-long single-short-dashed), and (5) the total internal potential energy of the Cl_3 system (solid). The averaging over the ensemble of 100 trajectories tends to smooth over the sharp peaks seen in individual trajectories (see Figure 3b and 4b) of individual solvent atom kinetic energy and of potential energy by which the energy is transferred through hard collisions, as these peaks occur at different times for different atoms and different trajectories.

is already excited, since the time scale for vibrational energy excitation and relaxation in rare gas solution is much longer.[1] The rotational motion is necessary for the proper, approximately linear, alignment of the diatomic with respect to the atom, whereas the translational and vibrational energies are both important in our case for the actual climbing of the barrier, as explained in the next section.

F. Reagent Barrier Climbing and Potential Energy. Armed with enough translational motion of the diatomic with respect to the atom and enough vibrational energy in the diatomic molecule, the system climbs the barrier in about 100 fs, as shown in Figure 7. In our system, where the barrier is symmetrically located with respect to the exit and entrance valleys, both vibrational and translational energies are important for climbing the barrier, although translation dominates. In other, unsymmetrical systems this will not necessarily be the case.[20] We observe that there is an interval of time around $t = 0$ in which the intramolecular forces within the Cl_3 reagents dominate the trajectories (as already noted in BRWH[1]), and the well-known gas-phase rules[35] for barrier crossing effectiveness of different types of reactant excitation will apply, even in liquid solution. In Figure 7 we plot the internal potential energy of the system of the three Cl atoms as a function of time, for an individual trajectory. The oscillations prior to the time when the barrier climbing occurs are due to the vibration of the diatomic.

G. Summary of Energy Flow. A clear picture of the energy fluctuations in the Cl + Cl_2 reaction in rare gas solvent can be seen from the results discussed above. In Figure 8 we summarize the time dependence of the different energy modes in the reacting system, averaged over 100 trajectories. We show as a function of time (1) the sum of the kinetic energies of the five atoms which did the most work, (2) the summed potential energy of these solvent atoms with respect to the reagent atoms, (3) the total work done by these solvent atoms on the reagent, (4) the total kinetic energy of the Cl_3 system (exclusive of the kinetic energy associated with translation of the center of mass), and (5) the total internal potential energy of the Cl_3 system. Note that the averaging over individual solvent atoms in a trajectory and the ensemble averaging smooths out the sharp spikes in the energy in the different modes as seen in the individual trajectories illustrated in Figure 3b, 4b, 5b, 6, and 7. From Figure 8 we can clearly see that there is a strong temporal correlation between the fluctuations in the different energy modes for those trajectories which are successful in reaching the top of the barrier and continuing to products. These mode fluctuations mark the energy flow from (i) solvent (mainly kinetic) thermal energy, into (ii) high kinetic energy of a few solvent atoms, peaking at around −200 fs, then into (iii) potential energy spikes due to hard solvent–reagent collisions as work is done by the few fast-moving solvent atoms on the reagents, peaking at around −125 fs, then into (iv) reactant kinetic energy[1] at around −75 fs, followed by (v) an "internal collision" between the reactants[1] converting their excess kinetic energy into the final potential energy to surmount the barrier at 0 fs.

IV. Conclusion

We have shown for a model A + BC atom-exchange reaction in rare gas solution that there is a particularly simple but revealing picture of energy flow from the solvent bath to the reaction system. We observe in our simulations the evolution of the fluctuation involved in climbing the barrier. This fluctuation begins with the energy in the solvent–reagent system distributed in an approximately equilibrium manner, even for those trajectories which will subsequently climb the barrier. Initially, these energy fluctuations must, in experimental reality, arise from a "heat wave" carrying energy in from the surrounding solution heat bath, producing a "hot spot" in the region of the reactants. (We assume that the A and BC are already near one another.) Then, in this particular reaction system, we find that excess kinetic energy appears in a few solvent atoms near the reactants. The next step is the transfer of the high kinetic energy from these few solvent atoms to the reactants via hard collisions which are seen as spikes in the potential energy between these atoms and the reactants. Armed with this energy, stored temporarily as reactant translational and rotational energies, as well as with vibrational energy already stored in the diatomic, the reactants collide with one another and convert the kinetic energy that they have gained into potential energy as they climb the barrier to reaction. The solvent atoms which participate in the fluctuation then return to equilibrium kinetic and potential energy distributions at the barrier top. Note that the predominant modes in which the energy is stored in this reaction are kinetic energy modes, and thus the "generalized" or "molecular dynamic" mechanism by which this reaction takes place is predominantly in the momentum part of phase space. This augments the usual views of reaction mechanism in solution[36] which are concerned with the evolution of atomic positions, and

(35) Levine, R. D.; Bernstein, R. B. *Molecular Reaction Dynamics and Chemical Reactivity*; Oxford University Press: New York, 1987.

(36) Lowry, T. H.; Richardson, K. S. *Mechanism and Theory in Organic Chemistry*, 3rd ed.; Harper and Row: New York, 1987.

thus focus on the coordinate part of phase space and much less on the role of momentum and kinetic energy.

The time scale of the energy fluctuation process (with the exception of vibrational energy, which is much longer) is seen to be ~250 fs. That it is so short can be understood by considering that in this particular reaction system, energy passes mainly through translational modes. As a general principle, the allowable time for the arising of a fluctuation will be limited by the time for its decay. For example, in our case a fluctuation producing translational excitation of nearby solvent atoms which occurred 5 ps before barrier climbing would not be useful, since the translational energy would have dissipated before it could be used for barrier climbing.

Acknowledgment. We thank J. T. Hynes, Antonio Liu, and John Rice for helpful dicussions. We also thank the National Science Foundation for supporting this work, both through research funds and a graduate fellowship to B.J.G.

Reaction-Surface Topography for Hydride Transfer: Ab Initio MO Studies of Isoelectronic Systems CH_3O^- + CH_2O and CH_3NH_2 + $CH_2NH_2^+$

Ian H. Williams,*[1a] Andrea B. Miller,[1b] and Gerald M. Maggiora*[1b]

Contribution from Upjohn Company, Kalamazoo, Michigan 49001, and the School of Chemistry, University of Bristol, Bristol BS8 1TS, U.K. *Received May 17, 1989*

Abstract: The topography of the transition-state regions of the multidimensional potential energy surfaces for hydride transfer, (1) from methylamine to methaniminium and (2) from methoxide to formaldehyde, is described qualitatively on the basis of the characteristics (relative energies and curvatures) of critical points, each having negative curvature in the potential along the hydride-transfer reaction coordinate. Several new critical points on the HF/3-21G surfaces are reported. The geometry of hydride transfer depends upon steric effects, electrostatic interactions, and the possibility of 2e or 6e transition-state aromaticity. The varying interplay of these factors accounts for the differences between the reaction surfaces of the isoelectronic systems considered.

The simplest chemical reactions may be represented within the Born–Oppenheimer approximation by potential energy (PE) surfaces containing a reagent valley (or minimum) separated from a product valley (or minimum) by a saddle region associated with a transition state: the archetypal example of collinear H + H_2 springs readily to mind. Discussions of rates and mechanisms of organic reactions, involving polyatomic reagents, may acknowledge the multidimensional nature of the corresponding PE hypersurfaces but often implicitly assume a similarly simple picture for each elementary step. The degenerate hydride transfer $A'H^- + A \rightarrow A' + HA^-$ might be imagined as a simple process involving a unique saddle point (‡) located between the reagent and product valleys (R and P) represented schematically by the contours in the horizontal plane of Figure 1. If ‡ were the only critical point occurring in the vertical dividing plane describing bent symmetrical structures, then the simple picture would indeed be valid. In this paper we show, however, that a degenerate hydride transfer as "simple" as that with A = A′ = CH_2O may be suprisingly complex. The dividing hyperplane of symmetrical structures orthogonal to the hydride-transfer reaction coordinate (HTRC) contains many critical points within a chemically significant range of energies.

We have chosen the example of hydride transfer since this class of reaction has been the subject of numerous recent theoretical studies, owing to its importance in organic chemistry and biochemistry.[2-11] The PE hypersurface for degenerate hydride transfer from methylamine to the methaniminium cation (reaction 1)[7,10] has just two geometrically distinct critical points in the dividing hyperplane between reagents and products, but the corresponding hyperplane for the isoelectronic methoxide anion–formaldehyde system (reaction 2)[2,8,9] contains six geometrically distinct critical points in the range of chemical significance, only three of which have been reported previously. We now show how the critical points in these dividing hyperplanes may be organized topographically by consideration not only of their indices (the numbers of imaginary vibrational frequencies) but also importantly of the nature of the corresponding normal modes. This strategy for mapping the chemically relevant critical points of model (but real) chemical reaction surfaces is particularly useful when these surfaces are of a gently undulating nature; to follow an intrinsic reaction coordinate (IRC) over such an essentially flat surface is very difficult. The specific details of this topographical investigation may change at higher levels of theory (e.g., larger basis sets and/or inclusion of electron correlation), but it is not our present aim to provide a quantitatively accurate description of these energy surfaces or a complete account of the chemical

(1) (a) SERC Advanced Fellow, University of Bristol. Present address: School of Chemistry, University of Bath, Bath BA2 7AY, U.K. (b) Upjohn Co.

(2) Sheldon, J. C.; Bowie, J. H.; Hayes, R. N. *Nouv. J. Chim.* **1984**, *8*, 79.

(3) Donkersloot, M. C. A.; Buck, H. M. *J. Am. Chem. Soc.* **1981**, *103*, 6549; *Ibid.* **1981**, *103*, 6554. Brounts, R. H. A. M.; Buck, H. M. *Ibid.* **1983**, *105*, 1284.

(4) van der Kerk, S. M.; van Gerresheim, W.; Verhoeven, J. W. *Recl. Trav. Chim. Pays-Bas* **1984**, *103*, 143. Verhoeven, J. W.; van Gerresheim, W.; Martens, F. M.; van der Kerk, S. M. *Tetrahedron* **1986**, *42*, 975.

(5) Rzepa, H. S.; Miller, J. *J. Chem. Soc., Perkin Trans. 2* **1985**, 717. Rajyaguru, I. H.; Rzepa, H. S. *J. Chem. Soc., Chem. Commun.* **1987**, 998.

(6) Tapia, O.; Andres, J.; Aullo, J. M.; Bränden, C.-I. *J. Chem. Phys.* **1985**, *83*, 4673. Tapia, O.; Cardenas, R.; Andres, J.; Colonna-Cesari, F. *J. Am. Chem. Soc.* **1988**, *110*, 4046.

(7) Hutley, B. G.; Mountain, A. E.; Williams, I. H.; Maggiora, G. M.; Schowen, R. L. *J. Chem. Soc., Chem. Commun.* **1986**, *267*; *Ibid.* 1303.

(8) Wu, Y.-D.; Houk, K. N. *J. Am. Chem. Soc.* **1987**, *109*, 906.

(9) Field, M. J.; Hillier, I. H.; Smith, S.; Vincent, M. A.; Mason, S. C.; Whittleton, S. N.; Watt, C. I. F.; Guest, M. F. *J. Chem. Soc., Chem. Commun.* **1987**, 84. Hillier, I. H.; Smith, S.; Mason, S. C.; Whittleton, S. N.; Watt, C. I. F.; Willis, J. *J. Chem. Soc., Perkin Trans. 2* **1988**, 1345.

(10) Wu, Y.-D.; Houk, K. N. *J. Am. Chem. Soc.* **1987**, *109*, 2226.

(11) Pain, A. E.; Williams, I. H. *J. Chem. Soc., Chem. Commun.* **1988**, 1367. Pain, A. E.; Williams, I. H. Manuscript in preparation.

0002-7863/90/1512-530$02.50/0